

GLOBAL FORTY-YEARS VALIDATION OF SEASONAL PRECIPITATION FORECASTS: ASSESSING EL NIÑO-DRIVEN SKILL

R. MANZANAS¹, M.D. FRÍAS², A.S. COFIÑO² and J.M. GUTIÉRREZ¹

Abstract. The skill of seasonal precipitation forecasts is assessed worldwide —grid point by grid point— for the forty-years period 1961–2000. To this aim, the ENSEMBLES multi-model hindcast is considered. Although predictability varies with region, season and lead-time, results indicate that 1) significant skill is mainly located in the tropics —20 to 40% of the total land areas—, 2) overall, SON (MAM) is the most (less) skillful season and 3) predictability does not decrease noticeably from one to four months lead-time —this is so especially in northern south America and the Malay archipelago, which seem to be the most skillful regions of the world—. An analysis of teleconnections revealed that most of the skillful zones exhibit significant teleconnections with El Niño. Furthermore, models are shown to reproduce similar teleconnection patterns to those observed, especially in SON —with spatial correlations of around 0.6 in the tropics—. Moreover, these correlations are systematically higher for the skillful areas. Our results indicate that the skill found might be determined to a great extent by the models' ability to properly reproduce the observed El Niño teleconnections, i.e., the better a model simulates the El Niño teleconnections, the higher its performance is.

1. Introduction

Seasonal forecasting is a promising research field with enormous impact on different socio-economic sectors such as water resources, agriculture, energy and health [see *Doblas-Reyes et al.*, 2013, and references therein]. Nowadays, seasonal forecasts are routinely produced by several institutions around the world using different global ocean-atmosphere coupled models. Moreover, these products are collected by a number of regional focal points worldwide to produce operational consensus seasonal forecasts with socio-economic potential —see, e.g., the Regional Climate Outlook Forum (RCOF) sponsored by the World Meteorological Organization (WMO), http://www.wmo.int/pages/prog/wcp/wcasp/clips/outlooks/climate_forecasts.html—. However, there are still several limiting factors which hinder the practical use of seasonal forecasts [see, e.g., *Goddard et al.*, 2010]. For instance, it is known that seasonal predictability strongly varies with the target variable, region and season [see, e.g., *Halpert and Ropelewski*, 1992; *van Oldenborgh*, 2004; *Barnston et al.*, 2010; *Doblas-Reyes, F. J. and Weisheimer, A. and Palmer, T. N. and Murphy, J. M. and Smith, D.*, 2010].

Therefore, in order to properly communicate the uncertainties related to seasonal predictions, it is needed to develop a comprehensive assessment of the performance of the different forecasting models worldwide, especially for those variables most widely used by the stakeholders and end-users. In particular, precipitation is the most challenging case for being less skillfully predicted than surface temperatures [see, e.g., *Barnston et al.*, 2010; *Doblas-Reyes, F. J. and Weisheimer, A. and Palmer, T. N. and Murphy, J. M. and Smith, D.*, 2010; *Bundel et al.*, 2011]. However, the majority of verification studies for seasonal forecasts of this variable have been conducted over limited areas of the world and for concrete seasons [see, e.g., *Batté and Déqué*, 2011; *Lim et al.*, 2011; *Kim et al.*, 2012a; *Landman and Beraki*, 2012]. A few studies have also been conducted worldwide [*van Oldenborgh et al.*, 2005; *Wang et al.*, 2009; *Barnston et al.*, 2010; *Doblas-Reyes, F. J. and Weisheimer, A. and Palmer, T. N. and Murphy, J. M. and Smith, D.*, 2010], using a number of validation scores —correlation, Ranked Probability Skill Score (RPSS) and Brier Skill Scores (BSS)—. However, the limited hindcast period available in the latter works

does not ensure a robust statistical validation. For instance, *Doblas-Reyes, F. J. and Weisheimer, A. and Palmer, T. N. and Murphy, J. M. and Smith, D.* [2010] analyzed the ENSEMBLES multi-model seasonal dataset, computing averaged scores over six large-scale regions of the world for the period 1991–2005.

In this paper we present a global —grid point by grid point— forty-years (1961–2000) robust validation of the ENSEMBLES multi-model seasonal hindcast —the longest-to-date available dataset of retrospective forecasts— by applying a simple tercile-based probabilistic validation scheme, obtaining a simple and easy to interpret —adequate for communication with decision-makers— measure of skill, the ROC Skill Score, which is the only skill score recommended by the Lead Centre for the Standardized Verification System (SVS) of Long Range Forecasts (LRF) <http://www.bom.gov.au/wmo/lrfvs/index.html> for the verification of probabilistic seasonal forecasts. One- and four-months lead predictions are considered for each of the four standard boreal seasons. Besides, since ENSO is known to be the major driving factor for seasonal predictability [*Goddard and Ditley*, 2005], we also analyze the El Niño-driven component of the skill in the different regions by assessing the ability of the models to properly reproduce the observed teleconnections. Thus, the two main goals of this study are 1) to fill the lack of an up-to-date user-oriented global validation of seasonal precipitation forecasts considering a long (forty years) period —identifying those regions of the world with significant skill— and 2) to analyze the El Niño-driven component of this skill, assessing to which extent predictability might be determined by this phenomenon.

The paper is organized as follows: The data used are described in Sec. 2. The methodology applied is explained in Sec. 3. Results are discussed through Sec. 4. Finally, the main conclusions are given in Sec. 5.

2. Data

On the one hand, VASclimO v1.1 [Beck *et al.*, 2005] was considered as the reference dataset for validation. This gauge-based product provides monthly precipitation totals on a 2.5° resolution grid for the global land areas (except the Antarctica) for the period 1951-2000. Fig. 1 shows the mean seasonal totals and the corresponding inter-annual standard deviation (STD) for this dataset for the period of study 1961-2000.

¹Grupo de Meteorología. Instituto de Física de Cantabria. CSIC-Univ. de Cantabria, Avda. de los Castros, s/n, 39005, Santander, Spain.

²Grupo de Meteorología. Dpto. Matemática Aplicada y Ciencias de la Computación. Univ. de Cantabria, Avda. de los Castros, s/n, 39005, Santander, Spain.

Copyright 2022 by the American Geophysical Union.
0148-0227/22/\$9.00

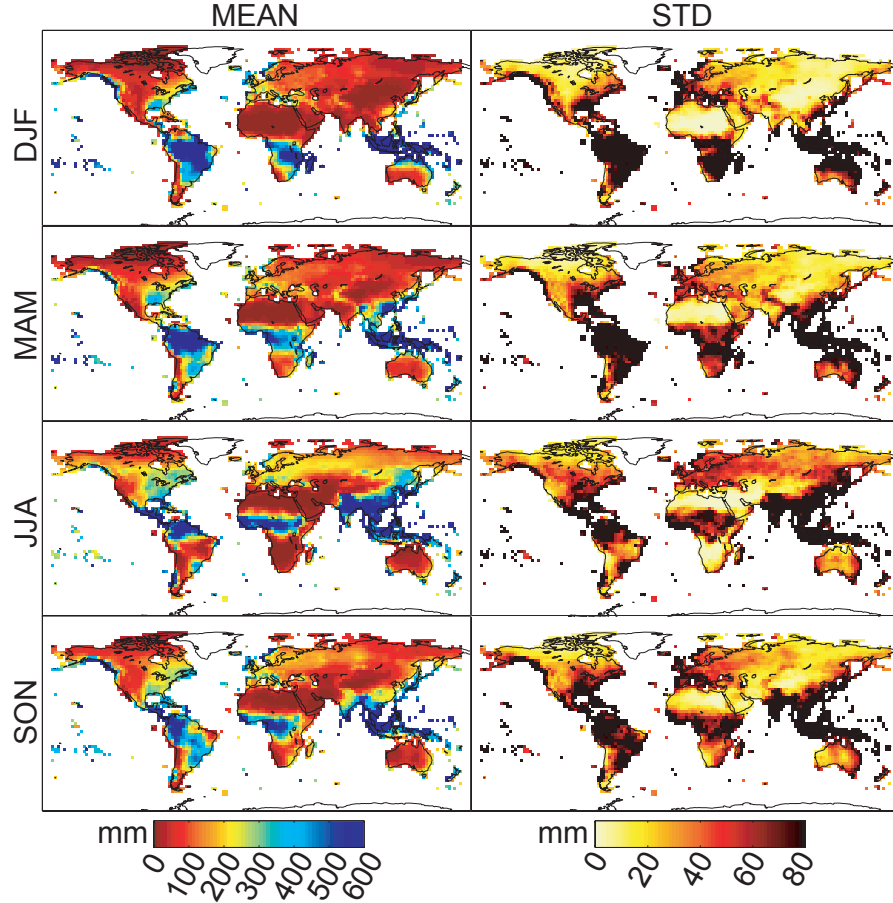


Figure 1. Mean and inter-annual standard deviation (left and right columns, respectively) of seasonal accumulated precipitation from VASclimO v1.1 for the four seasons considered (in rows) in the period 1961-2000.

In order to test the sensitivity to the reference data in the validation process, all calculations were also done for an alternative precipitation dataset, the Global Precipitation Climatology Centre full data reanalysis version 6 (GPCC v6) [Becker *et al.*, 2013]. The results obtained in both cases were very similar, thus only VASclimO v1.1 is considered hereafter.

On the other hand, predictions were obtained from the longest-to-date multi-model seasonal hindcast, provided by the EU project ENSEMBLES [Weisheimer *et al.*, 2009], which comprises five state-of-the-art atmosphere-ocean coupled models from the following centres: The UK Met Office (UKMO), Météo France (MF), the European Centre for Medium-Range Weather Forecasts (ECMWF), the Leibniz Institute of Marine Sciences (IFM-GEOMAR) and the Euro-Mediterranean

Centre for Climate Change (CMCC-INGV). Table 1 summarizes the main components of these models.

Table 1. Main components of the five state-of-the-art atmosphere-ocean coupled models contributing to the ENSEMBLES multi-model seasonal hindcast.

Centre	Atmospheric model and resolution	Ocean model and resolution
ECMWF	IFS CY31R1 (T159/L62)	HOPE (0.3° – 1.4°/L29)
IFM-GEOMAR	ECHAM5 (T63/L31)	MPI-OM1 (1.5°/L40)
CMCC-INGV	ECHAM5 (T63/L19)	OPA8.2 (2.0°/L31)
MF	ARPEGE4.6 (T63)	OPA8.2 (2.0°/L31)
UKMO	HadGEM2-A (N96/L38)	HadGEM2-O (0.33° – 1.0°/L20)

The atmosphere and the ocean were initialized using realistic estimates of their observed states and each model was run from an ensemble of nine initial conditions (nine equiprobable members). For each model, seven months-long runs were issued four times a year within the period 1960–2005, starting the first of February, May, August and November [see *Weisheimer et al.*, 2009, for more details about the experiment]. Thus, the seasons considered for validation were the standard boreal winter (DJF), spring (MAM), summer (JJA) and autumn (SON), since this allows to analyze one- and four-months lead predictions —e.g., the initializations of August and May can be used to forecast SON—. Note that although alternative three-months seasons could be more informative in particular regions of the world, there would be a single lead-time available for them, thus limiting the study. The validation period considered was 1961–2000, common to VASCLIM v1.1 observations and the ENSEMBLES models. All the models were bi-linearly interpolated to the grid of the observations —similar results were obtained using the nearest grid point interpolation technique (not shown)—.

3. Methodology

The validation methodology used in this work is the tercile-based probabilistic approach previously applied in other studies [see, e.g., *Frías et al.*, 2010; *Vellinga et al.*, 2013]. Thus, for each particular grid point and each particular model, member and season, the forty-years inter-annual series of predicted seasonal precipitation were categorized into three categories (dry, normal and wet), according to their respective climatological terciles within the period 1961–2000. Then, a probabilistic forecast was computed year by year by considering the number of members falling within each category, out of a total of $n = 9$ members. The terciles were defined independently for each model, considering

the inter-annual series of its nine members (a total of $40 \times 9 = 360$ values) —terciles were not computed at a member-level since no significant overlap among the dry and wet terciles of the nine members was found applying a Student’s t-test—. In the case of the multi-model (denoted hereafter as MM), $n = 45$ members were used to compute the probabilistic forecasts, thus assuming equal weights for all the models. In this case, the terciles were computed independently for each model. Note that working with precipitation categories instead of with raw values implicitly entails a bias correction grid point by grid point, which is required for a fair validation since the different models exhibit diverse season and region-dependent biases (not shown).

Rather than using deterministic scores [e.g., *van Oldenborgh et al.*, 2005; *Batté and Déqué*, 2011; *Lim et al.*, 2011; *Li et al.*, 2012; *Singh et al.*, 2012], the forecast performance is assessed in terms of a simple and easy to interpret measure of probabilistic skill [see *Jolliffe and Stephenson*, 2003, for an introduction to verification of probabilistic forecasts], the ROC Skill Score (ROCSS) [see, e.g., *Kharin and Zwiers*, 2003]. This score is a reasonable first choice to communicate the value of a forecast to the end-users [see, e.g. *Thiaw et al.*, 1999]. Moreover, it is the only skill score recommended by the Lead Centre for the Standardized Verification System (SVS) of Long Range Forecasts (LRF) <http://www.bom.gov.au/wmo/lrfvs/index.html> for the verification of probabilistic seasonal forecasts. The ROCSS is computed as $2A - 1$, where A is the area under the ROC curve (commonly used to evaluate the performance of probabilistic systems). For each tercile category (e.g., dry events), the ROC curve is drawn as the rate of occurrences correctly forecast (the Hit Rate, HIR_q) versus the rate of non-occurrences incorrectly forecast (the False Alarm Rate, FAR_q), as a function of a varying threshold q — q ranging from 0 to 1—. This threshold is used to convert the probabilistic prediction p into a binary deterministic one —the event is predicted to occur when $p > q$ —. The ROCSS ranges from 1 (perfect forecast

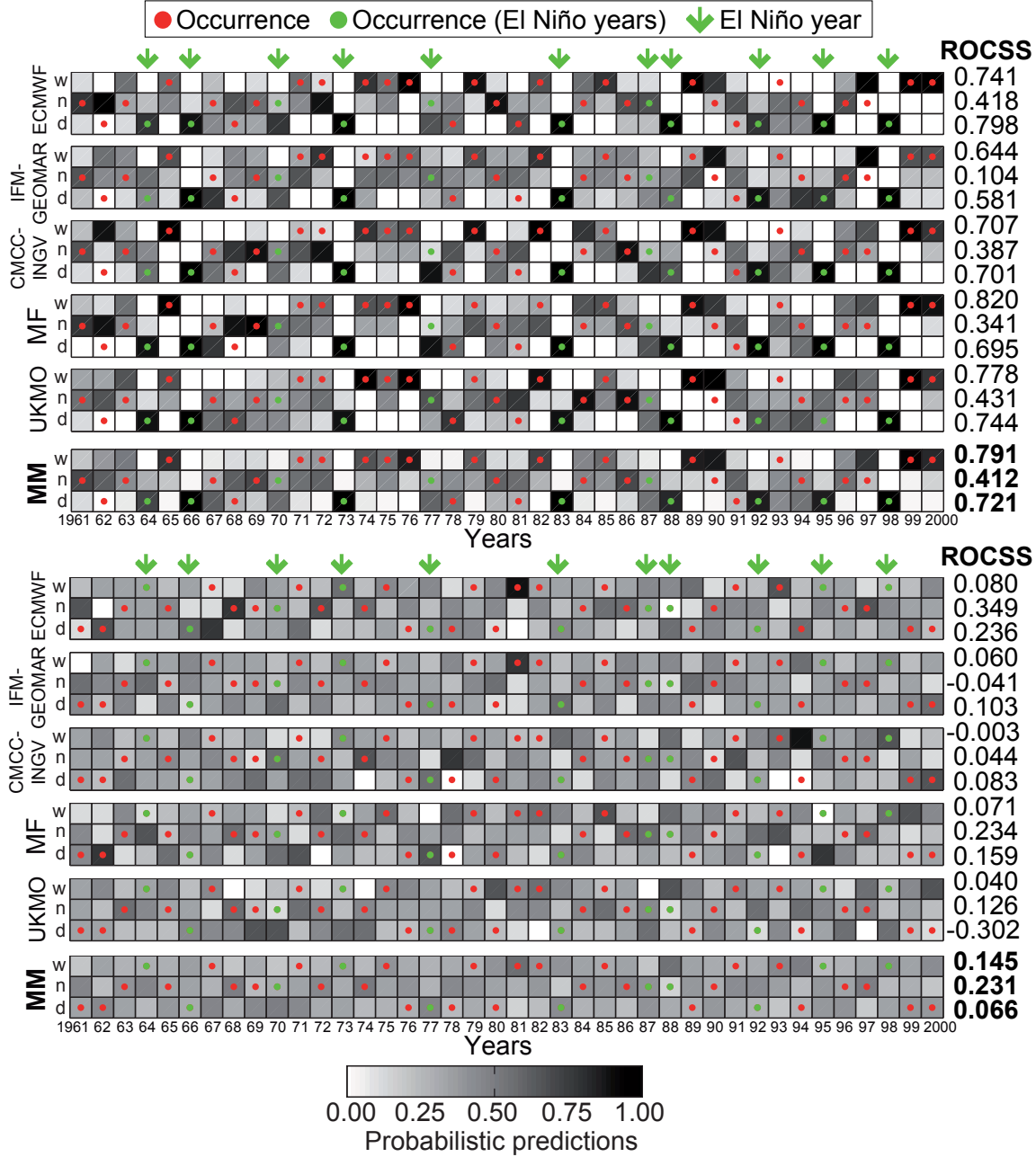


Figure 2. One-month lead probabilistic predictions from the five models and the MM for SON in an illustrative grid point in (top) the Malay archipelago —1.25° S, 121.5° E— and (bottom) Europe —51.25° N, 16.25° E—. For each tercile —*d*, *n* and *w* stand for dry, normal and wet, respectively—, probabilities are displayed in a white (0)-to-black (1) scale. Red (green) points mark the observed tercile in non-El Niño (El Niño) years —the latter are indicated by arrows—. Numbers on the right show the ROCSS for each model and terciles.

system) to -1 (perfectly wrong forecast system). A value zero indicates no skill with respect to a climatological prediction. In this work, the statistical significance of the ROCSS was obtained by bootstrapping [Mason and Graham, 2002] with 1000 samples, i.e., by generating 1000 time series of probabilistic forecasts by randomly re-sampling the original 1961-2000 sequence.

As an illustrative example of the validation scheme followed, Fig. 2 shows the 1961-2000 inter-annual time-series of probabilistic predictions from the five models

and the MM and the binary occurrence/non occurrence for the three terciles in two particular grid points — one in the Malay archipelago (top panel) and the other in Europe (bottom panel)— at one month lead-time for SON. Although varying from year to year and from model to model, predictions exhibit a higher resolution (probabilities far from 1/3) in the former point. Furthermore, resolution in this case increases in general in El Niño years (marked with green arrows), what suggests the existence of a predictability signal linked to

the latter phenomenon in this region of the world and for this season. Numbers on the right correspond to the ROCSS for the different models and terciles. High skill—over 0.7 in most of the cases—is found for the dry and wet terciles for the point in the Malay archipelago. On the contrary, almost no skill—ROCSS near to zero—is found for the point in Europe.

4. Results and Discussion

4.1. Overall Skill

We applied the above described methodology globally—grid point by grid point—in order to compute the ROCSS (and its corresponding significance) for the five models and the MM in the period 1961–2000, obtaining thus a measure of overall skill. As a summary of the results obtained, Fig. 3 shows the percentage of grid points with significant—at a 0.05 level—skill (over the total) in the land areas within the tropics—region in between 23.5° N and 23.5° S latitudes—and the extra-tropics, for both one- and four- months lead predictions. Although predictability varies with region,

season, model and lead-time, several general conclusions can be obtained. First, the skill concentrates in the extreme (wet or dry) terciles—similar levels are found for both—, whereas almost no signal is obtained for normal conditions (note that the percentage of significant grid points is around 5% in this case, which can be explained by chance according to the significance level considered). Second, predictability is mainly located in the tropics (20 to 40% of significant skillful grid points) rather than in the extra-tropics (only 10%), which is in agreement with previous studies [see, e.g., *van Oldenborgh et al.*, 2005]. Furthermore, SON (MAM) is the season exhibiting the highest (lowest) percentage of skillful areas in the former region. Third, all models yield similar results for a concrete region, season and lead-time, with the MM outperforming any of the single models in all cases, which is also in agreement with previous studies [see, e.g., *Doblas-Reyes et al.*, 2009; *Bundel et al.*, 2011; *Ma et al.*, 2012]. Finally, the percentage of skillful areas at four months lead-time do not decrease noticeably with respect to the one-month lead case in any season except MAM.

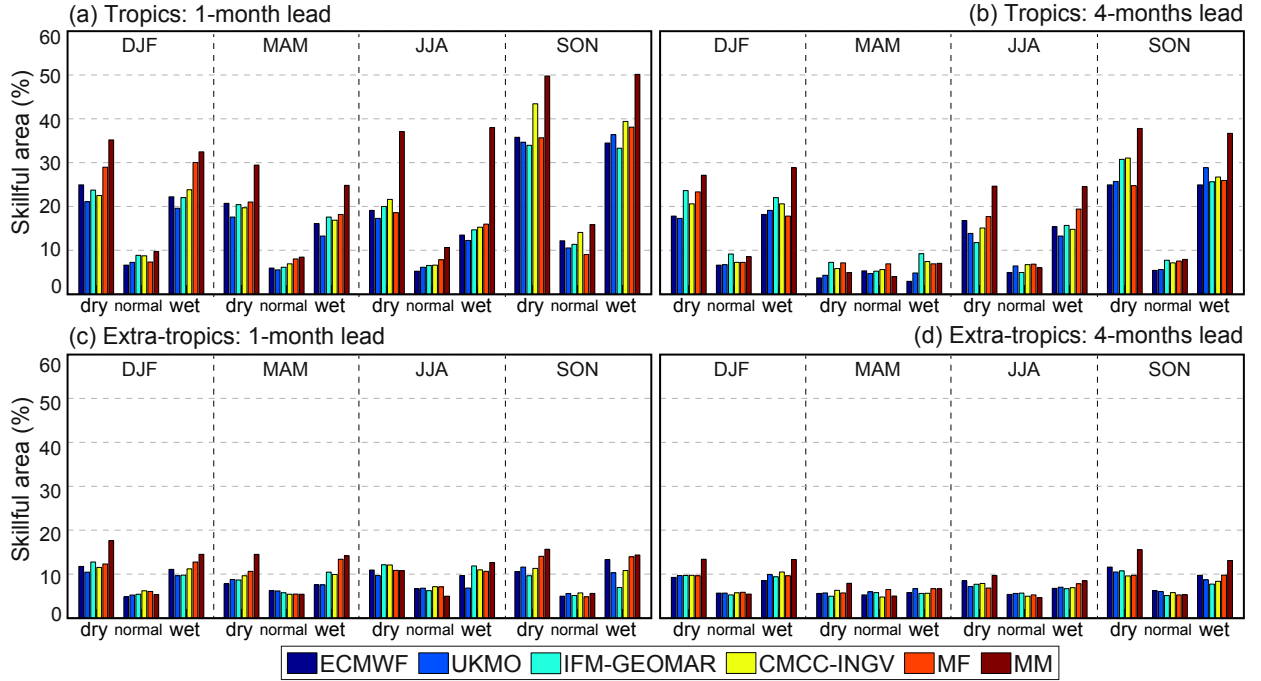


Figure 3. Percentage of land areas where significant—at a 5% level—ROCSS are obtained for one- and four-months lead predictions from the five models and the MM (see colors in legend) over the total in (a,b) the tropics and (c,d) the extra-tropics.

In order to further analyze the above results in the different regions of the world, global spatial maps of ROCSS were obtained for all the models and the MM.

Given its better performance, only results for the MM are reported in the following, for the sake of conciseness. Figs. 4 and 5 show the significant skill for the dry (left column) and wet (right column) terciles —almost no predictability is obtained for normal conditions— at one and four months lead-time, respectively, by seasons

(in rows). As can be seen, significant skill is mainly located over the tropics —being SON (MAM) the most (less) skillful season overall— and does not decrease noticeably from one to four months lead-time except in MAM (in agreement with Fig. 3).

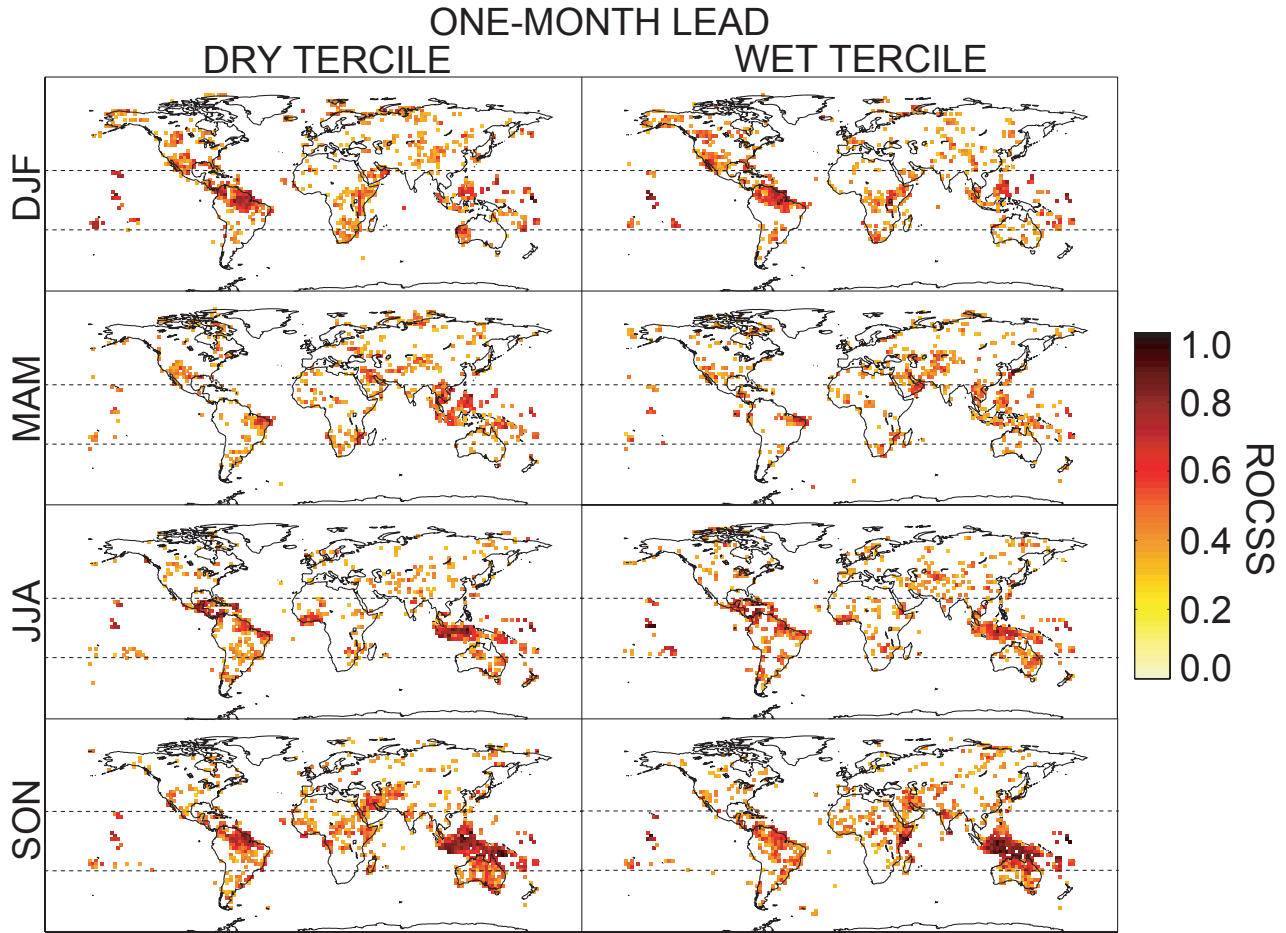


Figure 4. MM skill for the dry and wet (left and right columns, respectively) terciles at one month lead-time for the period 1961-2000, by seasons (in rows). Only significant —at a 5% level— ROCSS are shown. Dashed lines indicate the tropics/extra-tropics division.

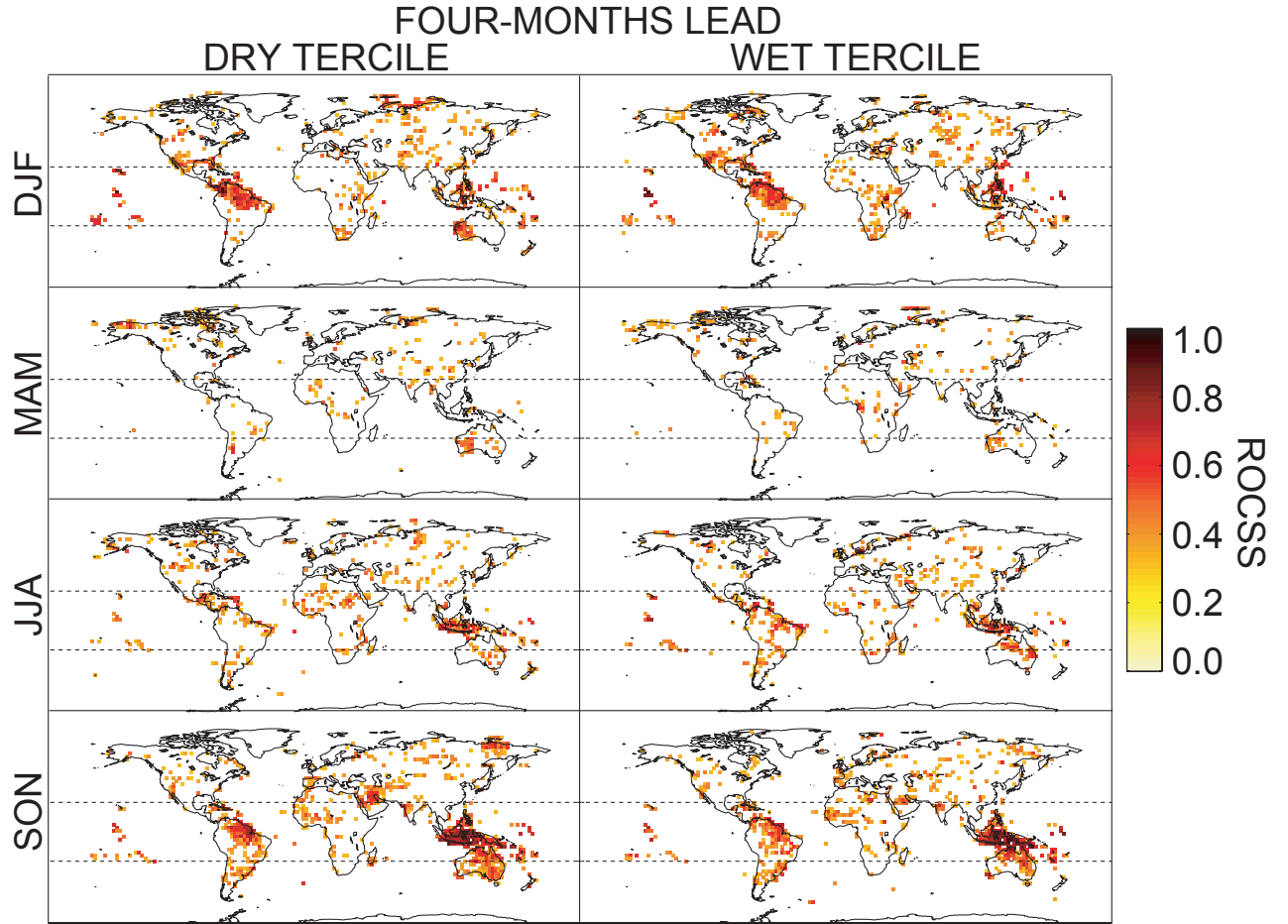


Figure 5. As Fig. 4, but for the four-months lead predictions.

By seasons, the main skillful regions at one month lead-time in DJF are the gulf of California, south America, central and southern Africa, western Australia and the Pacific islands of Oceania in Melanesia, Micronesia and Polynesia. Except in Africa, where the predictability signal weakens, most of this skill remains at four months lead-time. In MAM, skill at one month lead-time is located over parts of western U.S.A., northeastern Brazil, parts of the Arabic peninsula, Indochina and the Malay archipelago. However, most of this predictability vanishes at four months lead-time. In JJA, central America, northern Brazil, the gulf of Guinea, the Malay archipelago, eastern Australia and the Pacific islands of Oceania are the main skillful regions at one month lead-time. This skill is only maintained in the Malay archipelago and the Pacific islands of Oceania

at four months lead-time. Finally, one-month lead skill in SON is located over northern south America, a belt in central Africa (especially in the Somali peninsula), parts of Middle East, the Malay archipelago, Australia and the Pacific islands of Oceania. Moreover, this skill remains unaltered at four months lead-time for all the aforementioned regions except the Somali peninsula, indicating thus a strong predictability signal.

In the light of the previous results, northern south America and the Malay archipelago seem to be the most skillful regions of the world for seasonal forecasting of precipitation. Note that seasonal predictability in these regions has been analyzed in previous studies [Aldrian *et al.*, 2007; Haylock and McBride, 2001], considering also its derived socio-economic impacts [Kirono and Tapper, 1999].

Finally, it is noteworthy to mention that there is a symmetry in the ROCSS found for both dry and wet

terciles, leading to similar maps in both cases. The reason for this is that large dry (wet) HIR values partially contribute to low wet (dry) FAR values, since those dry (wet) events correctly forecast are also non-wet (non-dry) events correctly forecast. However, the reverse is not generally true; e.g., non-wet correct forecasts do not necessarily imply a correct forecast of the corresponding dry (or normal) event. From a practical point of view, the positive prediction of a particular event (dry or wet) is more valuable than its negative one (normal-wet or normal-dry, respectively). Thus, besides obtaining the ROCSS maps it is also important to understand the factors driving this skill and how they influence both dry and wet events. As we will see in the following section, this is regulated to a great extent by the El Niño phenomenon.

4.2. El Niño-Driven Skill

Despite the important achievements reached in seasonal forecasting in the last ten years, significant levels of skill for precipitation are only generally found over regions strongly connected with ENSO [see, e.g., *Coelho et al.*, 2006; *Barnston et al.*, 2010; *Arribas et al.*, 2011; *Lim et al.*, 2011; *Kim et al.*, 2012a, b; *Landman and Beraki*, 2012], which is known to be the dominant mode of seasonal variability [*Doblas-Reyes, F. J. and Weisheimer, A. and Palmer, T. N. and Murphy, J. M. and Smith, D.*, 2010]. The aim of this section is to analyze to which extent El Niño contributes to the

overall (1961-2000) skill found in Sec. 4.1. To this, we computed the observed El Niño teleconnections in order to look for a possible link between them and the seasonal predictability exhibited by the models —and consequently, the MM— (see Figs. 4 and 5). Teleconnections were also calculated following a tercile-based approach, in terms of the frequencies of occurrence of each category in El Niño periods —as compared with the climatological frequency $1/3$ —. The eleven El Niño years considered were the ones defined in *Pozo-Vázquez et al.* [2005] as *El Niño Winter* years: 1964, 1966, 1970, 1973, 1977, 1983, 1987, 1988, 1992, 1995 and 1998. Alternatively, we also considered *El Niño Autumn* years —defined as well *Pozo-Vázquez et al.* [2005]—, obtaining similar conclusions (not shown). A one-sample Z-test for proportions was applied to detect those frequencies significantly higher (lower) than $1/3$, which are considered as significant positive (negative) El Niño teleconnections. Fig. 6 shows the results obtained for the dry and wet terciles (left and right columns, respectively) in the different seasons (in rows). Red/blue for the dry (wet) tercile indicates those grid points where dry/normal-wet (wet/normal-dry) conditions are mainly observed in El Niño years. Overall, our results are in agreement with previous studies [see, e.g., *Ropelewski and Halpert*, 1987; *van Oldenborgh et al.*, 2000; *Kayano et al.*, 2009; *Shaman and Tziperman*, 2011; *Zhang et al.*, 2012; *Yadav et al.*, 2013; *Zhang et al.*, 2013].

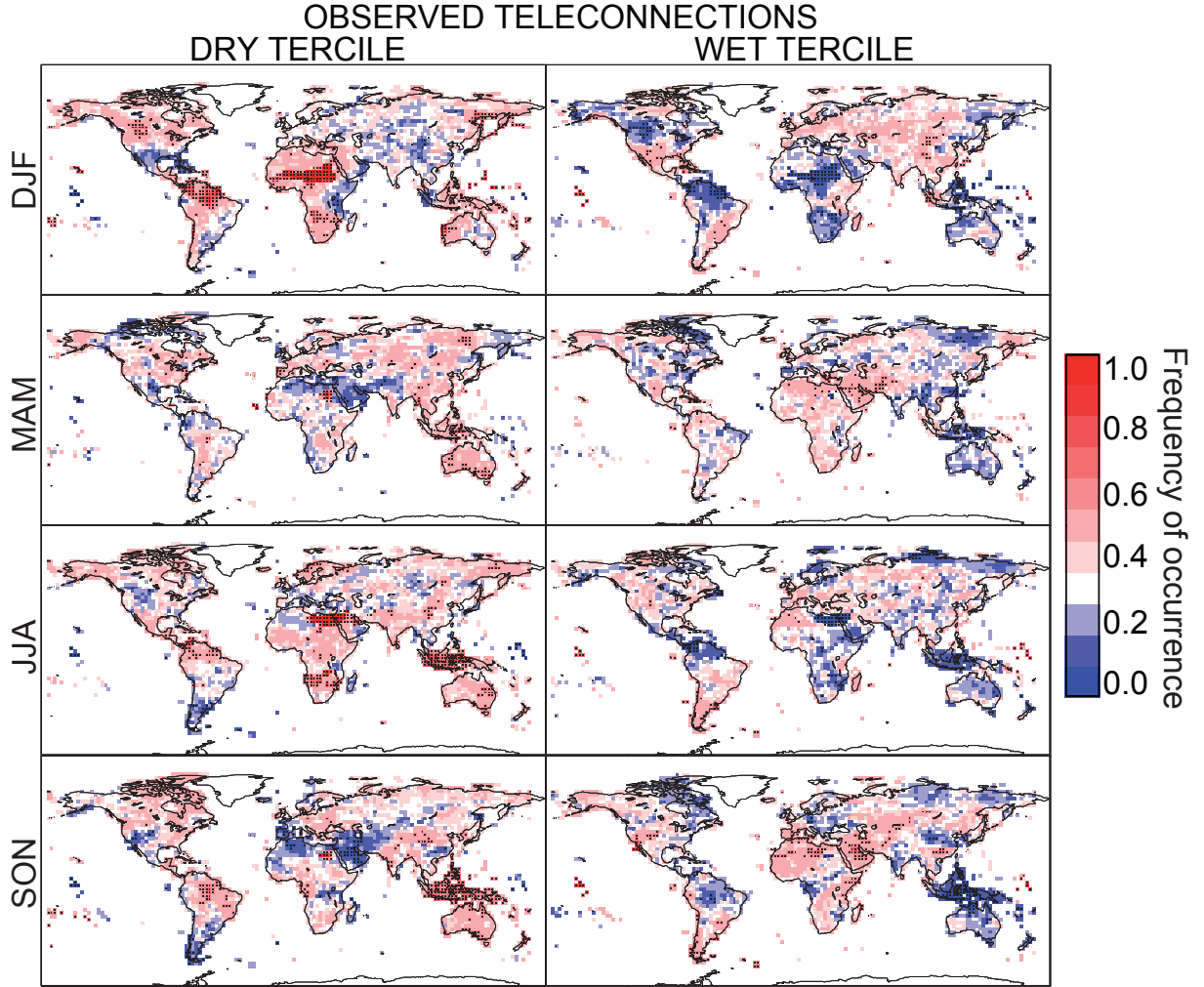


Figure 6. Relative frequency of occurrence for the dry and wet terciles (left and right columns, respectively) in El Niño years for the different seasons (in rows). Red (blue) colors correspond to values above (under) $1/3$, the expected climatological frequency. Black dots indicate significant —at a 5% level— teleconnections, according to a one-sample Z-test for proportions.

However, rather than analyzing the teleconnections in the different regions of the world, here we focus on the relationship between these teleconnection maps and those reporting the skill (Figs. 4 and 5). Visual inspection reveals that, in general, the skillful areas correspond to those significantly teleconnected with El Niño (black dots in Fig. 6), as occurs, for instance, in northern south America in DJF and SON and in Middle East and the Malay archipelago in SON. Moreover, there are no spatially consistent zones of skill which are not teleconnected with this phenomenon. This suggests that both the seasonal and spatial distribution of the over-

all skill can be accurately explained by the observed El Niño teleconnections, i.e., the skill found might have a strong El Niño-driven component.

Therefore, it is reasonable to think that the models' skill might be determined to a great extent by their ability to properly reproduce the observed El Niño teleconnections. To further analyze this fact, the teleconnections reproduced by the different models and the MM were computed and compared against the observed ones. Note that, although a similar analysis has been done in *Yang and Delsole* [2012], they did not relate their results to the models' performance, which is the aim here. As the observed ones, the simulated telecon-

nections were also computed in terms of the frequencies of occurrence of the different terciles in El Niño years—from a total of 11 (El Niño years) \times 9 (members) = 99 values for each single model and 11 (El Niño years) \times 45 (members) = 495 values for the MM—. Note that the independence assumption required by the Z-test does not hold in this case (members are not independent) and, thus, the significance of the results is not computed. Fig. 7 shows the resulting MM teleconnections for the one-month lead predictions (results are similar for the four months case). As can be seen, the predicted patterns are smoother than the observed

ones (this feature is less pronounced for the individual models) and are in good agreement with them (see Fig. 6)—numbers in each map show the spatial correlation between the observed and predicted patterns—. Furthermore, agreement is noticeable—correlations around 0.5—in the most skillful seasons (SON and DJF) whereas it is poor in the season with the lowest skill (MAM). These results confirm that the MM appropriately reproduce the observed teleconnections in the different skillful regions and, thus, that the overall skill found in Sec. 4.1 might be determined to a great extent by this ability.

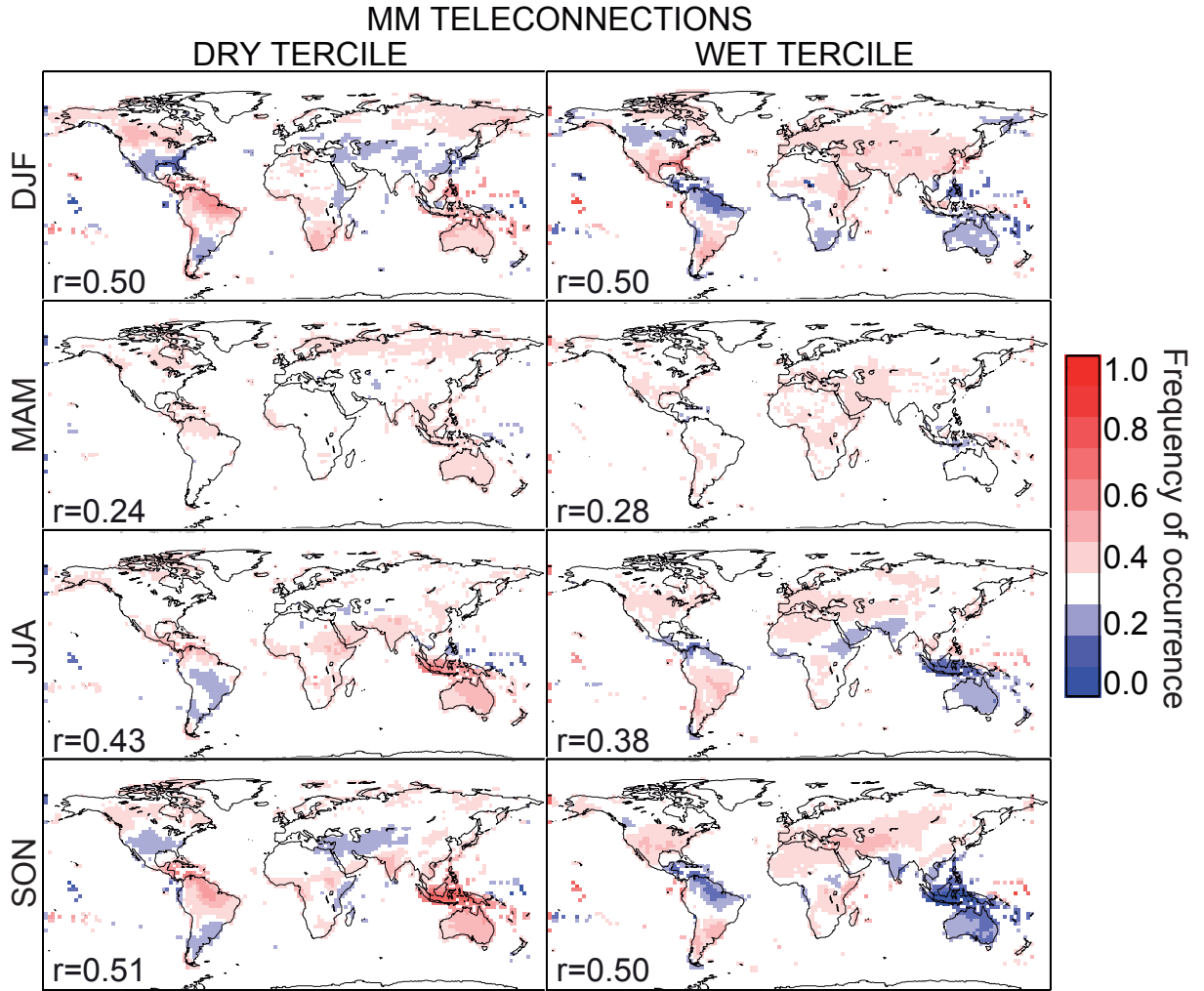


Figure 7. El Niño teleconnections reproduced by the MM for the dry and wet terciles (left and right columns, respectively) at one month lead-time. The numbers in each panel show the spatial correlation with the corresponding observed patterns (Fig. 6). Note that significance can not be calculated in this case since the independence assumption required by Z-test do not hold due to the interdependence among members within the same model.

In order to quantify this claim for the rest of models, Fig. 8 shows the spatial correlation between the observed and predicted —for one- and four-months lead forecasts (left and right panels, respectively)— teleconnections over (a,b) the entire tropics and (c,d) those tropical grid points exhibiting significant skill for the five single models and the MM (see colors in legend).

Results are consistent with the above argumentation, finding the highest (lowest) correlations in the most (less) skillful seasons, DJF and SON (MAM). Moreover, correlations are systematically higher when restricting the analysis to skillful grid points —e.g., values in SON increase from 0.6 to 0.8—. In addition, note that this figure is in very much agreement with the results obtained in terms of skillful areas (see Fig. 3a-b).

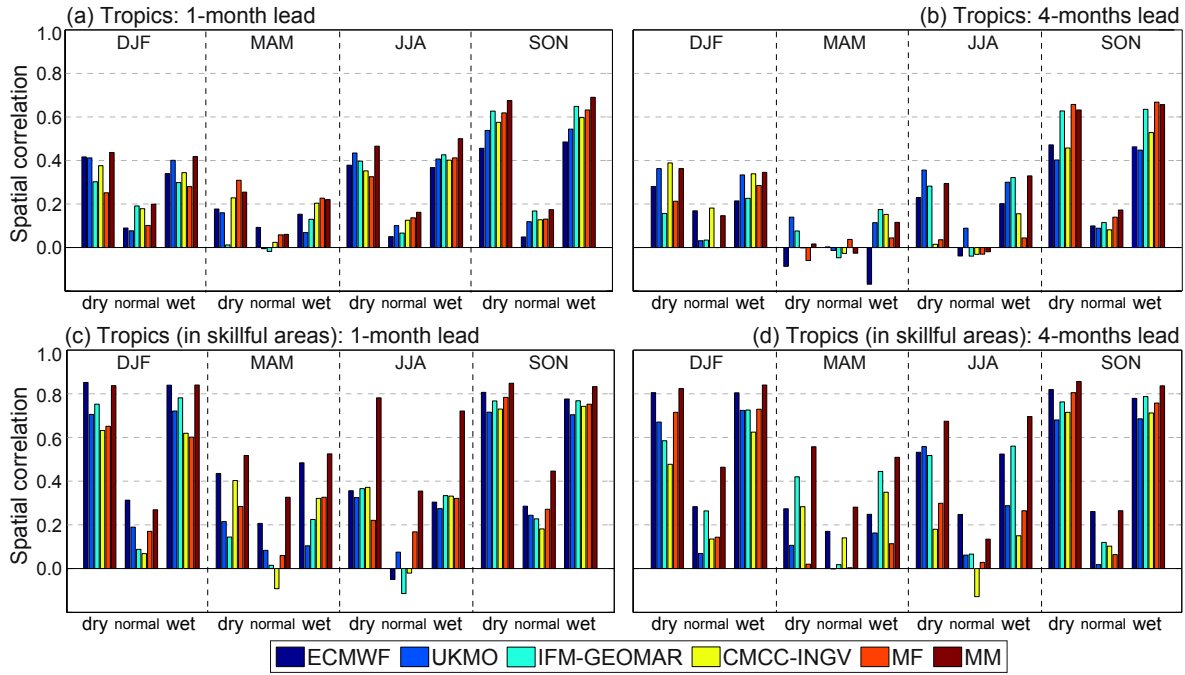


Figure 8. Spatial correlation between the observed and predicted El Niño teleconnection patterns in the tropics for (a,c) one- and (b,c) four-months lead seasonal predictions for the five models and the MM (see legend for colors). The panels in the top correspond to the entire tropics, whereas panels in the bottom correspond to those tropical grid points showing significant skill (see Figs. 4 and 5).

Finally, we want to mention that we also tried to quantify the contribution of the El Niño phenomenon to the skill by computing the ROCSS in the eleven El Niño years. However, the results turned out to be misleading due to the existence of unobserved tercile categories (e.g., dry events) in some grid points in El Niño periods. In these cases, the ROCSS can be only calculated for the normal and wet events and, thus, do not reflect the ability of the models to predict dry events. For instance, the skill obtained in Middle East in SON completely vanishes when conditioning the analysis to El Niño years (not shown), suggesting an alternative source of skill rather than El Niño for this region. However, the above results clearly show that the skill there is clearly driven by El Niño. Therefore, we want to warn on the use of the ROCSS in cases with small samples where some categories could remain unobserved.

5. Conclusions

The skill of seasonal precipitation forecasts has been assessed worldwide for the forty-years period 1961–2000. To this aim, the ENSEMBLES multi-model seasonal

hindcast was considered. A probabilistic tercile-based validation scheme was applied, obtaining the skill—in terms of the ROC Skill Score—and its statistical significance grid point by grid point. Although predictability varies with region, season and lead-time, results indicate that skill is mainly located in the tropics—with 20 to 40% of significant skillful areas—rather than in the extra-tropics—only around the 10%. Overall, DJF and SON (MAM) are the most (less) skillful seasons. In particular, seasonal predictability is especially strong in SON, where the skill found over northern south America, a belt in central Africa, parts of Middle East, the Malay archipelago, Australia and the Pacific islands of Oceania at one month lead-time remains almost unaltered at four-months lead.

The extent to which El Niño contributes to the latter skill was evaluated by means of an analysis of teleconnections. Results reveal that skillful areas are essentially those significantly teleconnected with El Niño, what suggest that the skill found might be driven by this phenomenon. To further analyze this, the performance of the different models to reproduce the El Niño teleconnections was assessed by computing the spatial correlation between the observed and predicted telecon-

nection patterns. The highest correlations (around 0.6 in the tropics) are found in SON, whereas the lowest (nearly negligible) are found in MAM—the most and less skillful seasons, respectively—. Moreover, the latter correlations are systematically higher (over 0.8) when restricting the analysis to the skillful areas. These results indicate that the seasonal and spatial distribution of the skill can be explained to a great extent by the model's ability to properly reproduce the observed El Niño teleconnections.

Acknowledgments. This study was supported by the EU projects QWeCI and SPECS, funded by the European Commission Seventh Framework Research Programme under grant agreements 243964 and 308378, respectively. The authors want also to acknowledge the ENSEMBLES project, funded by the European Commission Sixth Framework Research Programme through contract GOCE-CT-2003-505539, for the data models' data, which were retrieved from the Meteorological Archival and Retrieval System (MARS) of the ECMWF, <http://www.ecmwf.int/services/archive/>.

References

- Aldrian, E., L. Dümenil Gates, and F. H. Widodo (2007), Seasonal variability of Indonesian rainfall in ECHAM4 simulations and in the reanalyses: The role of ENSO, *Theoretical and Applied Climatology*, 87(1-4), 41–59, doi:10.1007/s00704-006-0218-8.
- Arribas, A., M. Glover, A. Maidens, K. Peterson, M. Gordon, C. MacLachlan, R. Graham, D. Fereday, J. Camp, A. A. Scaife, P. Xavier, P. McLean, A. Colman, and S. Cusack (2011), The GloSea4 ensemble prediction system for seasonal forecasting, *Monthly Weather Review*, 139(6), 1891–1910, doi:10.1175/2010MWR3615.1.
- Barnston, A. G., S. Li, S. J. Mason, D. G. Dewitt, L. Goddard, and X. Gong (2010), Verification of the first 11 years of IRI's seasonal climate forecasts, *Journal of Applied Meteorology and Climatology*, 49(3), 493–520, doi:10.1175/2009JAMC2325.1.
- Batté, L., and M. Déqué (2011), Seasonal predictions of precipitation over Africa using coupled ocean-atmosphere general circulation models: Skill of the ENSEMBLES project multimodel ensemble forecasts, *Tellus A*, 63(2), 283–299, doi:10.1111/j.1600-0870.2010.00493.x.
- Beck, C., J. Grieser, and B. Rudolf (2005), A new monthly precipitation climatology for the global land areas for the period 1951 to 2000, *Tech. rep.*, Klimastatusbericht.
- Becker, A., P. Finger, A. Meyer-Christoffer, B. Rudolf, K. Schamm, U. Schneider, and M. Ziese (2013), A description of the global land-surface precipitation data products of the Global Precipitation Climatology Centre with sample applications including centennial (trend) analysis from 1901-present, *Earth System Science Data*, 5(1), 71–99, doi:10.5194/essd-5-71-2013.
- Bundel, A. Y., V. N. Kryzhov, Y. M. Min, V. M. Khan, R. M. Vilfand, and V. A. Tishchenko (2011), Assessment of probability multimodel seasonal forecast based on the APCC model data, *Russian Meteorology and Hydrology*, 36(3), 145–154, doi:10.3103/S1068373911030010.
- Coelho, C. A. S., D. B. Stephenson, F. J. Doblas-Reyes, and M. Balmaseda (2006), The skill of empirical and combined/calibrated coupled multi-model South American seasonal predictions during ENSO, *Advances in Geosciences*, 6, 51–55, doi:10.5194/adgeo-6-51-2006.
- Doblas-Reyes, F. J., A. Weisheimer, A. Déqué, N. Keenlyside, M. MacVean, J. M. Murphy, P. Rogel, D. Smith, and T. N. Palmer (2009), Addressing model uncertainty in seasonal and annual dynamical ensemble forecasts, *Quarterly Journal of the Royal Meteorological Society*, 135(643), 1538–1559, doi:10.1002/qj.464.
- Doblas-Reyes, F. J., J. García-Serrano, F. Lienert, A. P. Bescas, and L. R. L. Rodrigues (2013), Seasonal climate predictability and forecasting: Status and prospects, *Wiley Interdisciplinary Reviews: Climate Change*, 4(4), 245–268, doi:10.1002/wcc.217.
- Doblas-Reyes, F. J. and Weisheimer, A. and Palmer, T. N. and Murphy, J. M. and Smith, D. (2010), Forecast quality assessment of the ENSEMBLES seasonal-to-decadal Stream 2 hindcasts, *Tech. Rep. 621*, European Centre for Medium-Range Weather Forecasts (ECMWF).
- Friás, M. D., S. Herrera, A. S. Cofiño, and J. M. Gutiérrez (2010), Assessing the skill of precipitation and temperature seasonal forecasts in Spain. Windows of opportunity related to ENSO events, *Journal of Climate*, 23(2), 209–212, doi:10.1175/2009JCLI2824.1.
- Goddard, L., and M. Dilley (2005), El Niño: Catastrophe or opportunity, *Journal of Climate*, 18(5), 651–665, doi:10.1175/JCLI-3277.1.
- Goddard, L., Y. Aitchellouche, W. Baethgen, M. Dettinger, R. Graham, P. Hayman, M. Kadi, R. Martínez, and H. Meinke (2010), Providing seasonal-to-interannual climate information for risk management and decision-making, *Procedia Environmental Sciences*, 1(0), 81 – 101, doi:10.1016/j.proenv.2010.09.007.
- Halpert, M. S., and C. F. Ropelewski (1992), Surface temperature patterns associated with the Southern Oscillation, *Journal of Climate*, 5(6), 577–593, doi:10.1175/1520-0442(1992)005<0577:STPAWT>2.0.CO;2.
- Haylock, M., and J. McBride (2001), Spatial coherence and predictability of Indonesian wet season rainfall, *Journal of Climate*, 14(18), 3882–3887.
- Jolliffe, I. T., and D. B. Stephenson (2003), *Forecast verification: A practitioner's guide in atmospheric sciences*, John Wiley & Sons.
- Kayano, M. T., C. P. de Oliveira, and R. V. Andreoli (2009), Interannual relations between South American rainfall and tropical sea surface temperature anomalies before and after 1976, *International Journal of Climatology*, 29(10), 1439–1448.
- Kharin, V. V., and F. W. Zwiers (2003), On the ROC score of probability forecasts, *Journal of Climate*, 16(24), 4145–4150, doi:10.1175/1520-0442(2003)016<4145:OTRSOP>2.0.CO;2.
- Kim, H. M., P. J. Webster, and J. A. Curry (2012a), Seasonal prediction skill of ECMWF System 4 and NCEP CFSv2 retrospective forecast for the Northern Hemisphere winter, *Climate Dynamics*, 39(12), 2957–2973, doi:10.1007/s00382-012-1364-6.
- Kim, H. M., P. J. Webster, J. A. Curry, and V. E. Toma (2012b), Asian summer monsoon prediction in ECMWF System 4 and NCEP CFSv2 retrospective seasonal forecasts, *Climate Dynamics*, 39(12), 2975–2991, doi:10.1007/s00382-012-1470-5.
- Kirono, D. G. C., and N. J. Tapper (1999), ENSO rainfall variability and impacts on crop production in Indonesia, *Physical Geography*, 20(6), 508–519, doi:10.1080/02723646.1999.10642693.
- Landman, W. A., and A. Beraki (2012), Multi-model forecast skill for mid-summer rainfall over southern Africa, *International Journal of Climatology*, 32(2), 303–314, doi:10.1002/joc.2273.
- Li, C., R. Lu, and B. Dong (2012), Predictability of the western North Pacific summer climate demonstrated by the coupled models of ENSEMBLES, *Climate Dynamics*, 39(1-2), 329–346, doi:10.1007/s00382-011-1274-z.
- Lim, E. P., H. H. Hendon, D. L. T. Anderson, A. Charles, and O. Alves (2011), Dynamical, statistical-dynamical, and multimodel ensemble forecasts of Australian spring season rainfall, *Monthly Weather Review*, 139(3), 958–975, doi:10.1175/2010MWR3399.1.
- Ma, S., X. Rodó, and F. J. Doblas-Reyes (2012), Evaluation of the DEMETER performance for seasonal hindcasts of the Indian summer monsoon rainfall, *International Journal of Climatology*, 32(11), 1717–1729, doi:10.1002/joc.2389.
- Mason, S. J., and N. E. Graham (2002), Areas beneath the relative operating characteristics (ROC) and relative operating levels (ROL) curves: Statistical significance and interpretation, *Quarterly Journal of the Royal Meteorological Society*, 128, 2145–2166, doi:10.1256/003590002320603584.
- Pozo-Vázquez, D., S. R. Gámiz-Fortis, J. Tovar-Pescador, M. J. Esteban-Parra, and Y. Castro-Díez (2005), El Niño-Southern Oscillation events and associated European winter precipitation anomalies, *International Journal of Climatology*, 25(1), 17–31, doi:10.1002/joc.1097.

- Ropelewski, C. F., and M. S. Halpert (1987), Global and regional scale precipitation patterns associated with the El Niño/Southern Oscillation, *Monthly Weather Review*, *115*(8), 1606–1626, doi:10.1175/1520-0493.
- Shaman, J., and E. Tziperman (2011), An atmospheric teleconnection linking ENSO and Southwestern European precipitation, *Journal of Climate*, *24*(1), 124–139, doi:10.1175/2010JCLI3590.1.
- Singh, A., N. Acharya, U. C. Mohanty, A. W. Robertson, and G. Mishra (2012), On the predictability of Indian summer monsoon rainfall in general circulation model at different lead time, *Dynamics of Atmospheres and Oceans*, *58*, 108–127, doi:10.1016/j.dynatmoce.2012.09.004.
- Thiaw, W. M., A. G. Barnston, and V. Kumar (1999), Predictions of African rainfall on the seasonal timescale, *Journal of Geophysical Research D: Atmospheres*, *104*(D24), 31,589–31,597, doi:10.1029/1999JD900906.
- van Oldenborgh, G. J. (2004), Assessing the skill of seasonal forecasts, *Tech. rep.*, KNMI Research Biennial Reports.
- van Oldenborgh, G. J., G. Burgers, and A. K. Tank (2000), On the El Niño teleconnection to spring precipitation in Europe, *International Journal of Climatology*, *20*(5), 565–574, doi:10.1002/(SICI)1097-0088(200004)20:5<565::AID-JOC488>3.0.CO;2-5.
- van Oldenborgh, G. J., M. A. Balmaseda, L. Ferranti, T. N. Stockdale, and D. L. T. Anderson (2005), Evaluation of atmospheric fields from the ECMWF seasonal forecasts over a 15 year period, *Journal of Climate*, *18*(16), 3250–3269, doi:10.1175/JCLI3421.1.
- Vellinga, M., A. Arribas, and R. Graham (2013), Seasonal forecasts for regional onset of the West African monsoon, *Climate Dynamics*, *40*(11–12), 3047–3070, doi:10.1007/s00382-012-1520-z.
- Wang, B., J. Y. Lee, I. S. Kang, J. Shukla, C. K. Park, A. Kumar, J. Schemm, S. Cocke, J. S. Kug, J. J. Luo, T. Zhou, B. Wang, X. Fu, W. T. Yun, O. Alves, E. K. Jin, J. Kinter, B. Kirtman, T. Krishnamurti, N. C. Lau, W. Lau, P. Liu, P. Pegion, T. Rosati, S. Schubert, W. Stern, M. Suarez, and T. Yamagata (2009), Advance and prospectus of seasonal prediction: Assessment of the APCC/ CliPAS 14-model ensemble retrospective seasonal prediction (1980–2004), *Climate Dynamics*, *33*(1), 93–117, doi:10.1007/s00382-008-0460-0.
- Weisheimer, A., F. J. Doblas-Reyes, T. N. Palmer, A. Alessandri, A. Arribas, M. Déqué, N. Keenlyside, M. MacVean, A. Navarra, and P. Rogel (2009), ENSEMBLES: A new multi-model ensemble for seasonal-to-annual prediction. Skill and progress beyond DEMETER in forecasting tropical pacific SSTs, *Geophysical Research Letters*, *36*, doi:10.1029/2009GL040896.
- Yadav, R. K., D. A. Ramu, and A. P. Dimri (2013), On the relationship between ENSO patterns and winter precipitation over North and Central India, *Global and Planetary Change*, *107*, 50–58, doi:10.1016/j.gloplacha.2013.04.006.
- Yang, X., and T. Delsole (2012), Systematic comparison of ENSO teleconnection patterns between models and observations, *Journal of Climate*, *25*(2), 425–446, doi:10.1175/JCLI-D-11-00175.1.
- Zhang, Q., J. Li, V. P. Singh, C. Y. Xu, and J. Deng (2013), Influence of ENSO on precipitation in the East River basin, South China, *Journal of Geophysical Research D: Atmospheres*, *118*(5), 2207–2219, doi:10.1002/jgrd.50279.
- Zhang, Y., Y. Qian, V. Dulière, E. P. Salathé Jr., and L. R. Leung (2012), ENSO anomalies over the Western United States: Present and future patterns in regional climate simulations, *Climatic Change*, *110*(1–2), 315–346, doi:10.1007/s10584-011-0088-7.

Corresponding author: R. Manzanás

Grupo de Meteorología. Instituto de Física de Cantabria. CSIC-Univ. de Cantabria, Avda. de los Castros, s/n, 39005, Santander, Spain

Email: rmanzanás@ifca.unican.es